

## Investigation on the Strengthening and Toughening Mechanism of 500 MPa V-Nb Microalloyed Anti-Seismic Rebars

Wei CHEN<sup>1,2</sup>, Jianchun CAO<sup>1\*</sup>, Yinhui YANG<sup>1</sup>, Zhe SHI<sup>2</sup>, Weiqiang ZHANG<sup>2</sup>,  
Min HUANG<sup>1</sup>

<sup>1</sup> Kunming University of Science and Technology, Kunming 650093, China

<sup>2</sup> Technology Center of WuKun Steel Co. Ltd., Kunming 650302, China

**crossref** <http://dx.doi.org/10.5755/j01.ms.21.4.9710>

Received 28 January 2015; accepted 21 October 2015

Two types of 500 MPa anti-seismic rebars were produced by V-Nb microalloyed combined with controlled rolling and cooling technology, the strengthening and toughening mechanism of which were investigated. The complex phase microstructures of specimens consist of ferrite, pearlite and bainite (6 – 10 %). Furthermore, a large number of V(C,N) and Nb(C,N) precipitates with size of 5 – 30 nm formed in the ferrite matrix, grain boundaries and on dislocation lines, promoting the precipitation strengthening and inhibiting grain coarsening to controlled cooling microstructure. The mechanical performance of the steels was improved by solution and grain refinement strengthening, precipitation and microstructure strengthening. And the best strengthening effect was obtained by grain refinement, which increased the yield strength more than 35 % strength increment contribution ratio to yield strength. Moreover, about 16.5 % microstructure strengthening increment was obtained due to bainite formation. The plasticity and low-temperature toughness enhancement were mainly attributed to ferrite grain refinement improvement.

**Keywords:** strengthening mechanism, steels, grain refinement, precipitation.

### 1. INTRODUCTION

The anti-seismic performance of rebar in reinforced concrete is the major cause of the improvement of today's structures, especially for those exposed to earthquake attacking regions. More recently, the amount of high-rise building increase rapidly with increasing population in the city, which need higher strength grade anti-seismic rebar to improve structure performance. Compared to 300 and 400 MPa rebar, 500 MPa anti-seismic rebar has obviously higher strength, larger safety reserves and better seismic behavior, which have been gradually used for high-rise and long-span building structure as new efficient building materials [1].

High strength and good toughness of anti-seismic rebar can be achieved by a combination of microalloyed and controlled rolling technology for factory production. It is well known that high strength mechanical property has been obtained with Nb, V and Ti addition in high-strength steel by effect of precipitation strengthening [2]. However, Ti oxide inclusions formed easily and become coarsening during steel smelting, lowering the mechanical property of steel. Meanwhile, the enhancing effects in strength were obtained by precipitation strengthening through microalloying with Nb and V individually or in combination [3–6]. R. Anumolua reported that niobium-microalloyed steels were characterized by similar yield strength but with the difference in impact toughness [7]. Klaus Hulka investigated the effect of niobium microalloying on strength of cold rolled Transformation-Induced Plasticity

(TRIP) steel, indicating that an increase in strength was achieved predominately by grain refinement and precipitation hardening [8]. S. Sankaran studied the tensile properties of three types of vanadium microalloyed medium carbon steels, indicating that the addition up to 0.14 wt.% V decreased the yield strength and work hardening rate significantly and improved the total elongation [9]. This can be related to a decrease in the amount of free carbon and nitrogen due to precipitation of vanadium carbide (VC) or vanadium nitride (VN). On the other hand, the addition of Nb and V has a large influence on microstructure and mechanical properties of high-strength low-alloy steels through the retardation of recovery and recrystallization and suppression of grain growth by small size precipitation formation during hot deformation. Some researchers introduced accelerating cooling as the core of new generation thermomechanical control process (TMCP) technology, which has been applied in steel production and improved the steel performance [10, 11]. Riccardo et al. reported that many carbonitride particles precipitates can be obtained in ferritic matrix by controlling appropriate final cooling temperature after finish rolling, which is beneficial to inhibit bainite grain growth after phase transformation and enhance the effect of the second-phase precipitation strengthening [12]. However, there are very limited data regarding the strengthening and toughening mechanism of V-Nb microalloyed anti-seismic rebars.

The controlled rolling and cooling microstructure and mechanical property of 500 MPa high-strength anti-seismic rebars with different V-Nb microalloyed processes were presented in this study. In order to better understand effect of V-Nb microalloyed combined with controlled

\* Corresponding author. Tel.: + 86 13187889483, fax: 087165109953,  
E-mail address: nmcjc@163.com (J.C. CAO)

rolling and cooling technology on 500 MPa anti-seismic rebars, the strengthening and toughening mechanism are further investigated.

## 2. EXPERIMENTAL DETAILS

Fig. 1 shows three rolling procedures by controlled rolling technology, and the controlled rolling and cooling procedure of tested steels are illustrated in the right procedure. The billet was rolled by 18-rack full continuous bar mill in steel rolling plant at temperature ranging from 990 to 1030 °C after reheating by regenerative heating furnace. The rough rolling procedure experienced six passes for 40–60 seconds and the medium rolling experienced 5–6 passes for 60–80 seconds. The pre-cooling devices were used after intermediate rolling and the amount of cooling water was controlled at 40–60 m<sup>3</sup>/h. Finally, the finish rolling performed 2–6 passes at the speed of 8.0–15.0 m/s for 45–65 seconds. The finish rolling temperature was controlled at temperatures of 850–900 °C and the controlled cooling process was taken after finish rolling. The steel bars were rapidly cooled with the cooling water flow of 260–300 m<sup>3</sup>/h and the termination temperature after controlled cooling was higher than 730 °C, and then were cooled in the air to room temperature. At last, the 500 MPa different V-Nb microalloyed high-strength anti-seismic rebars can be obtained. The chemical compositions of the steel bars with nominal diameters of 18 mm and 22 mm, represented as 1# and 2#, respectively, are shown in Table 1.

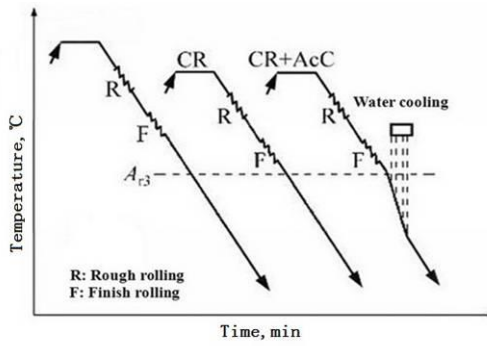


**Fig. 1.** Schematic illustration of different rolling procedures for controlled rolling and cooling technology (CR – controlled rolling; AcC CR – controlled cooling)

**Table 1.** Chemical composition of the tested material (wt.%)

Steel No.	C	Si	Mn	V	Nb	N	Fe
1#	0.21	0.42	1.42	0.029	0.019	0.0094	Bal.
2#	0.23	0.46	1.48	0.032	0.018	0.0105	Bal.

In order to investigate the mechanical properties, the samples of 400 CR–450 mm length cut from tested rebars were performed by tensile testing machine according to Chinese GB/T 228 CR–2002 at room temperature. The sample of center region with 2 mm radius and the sample of outer layer region from two-thirds of transversal section center for tested rebar were cut by wire-electrode cutting respectively, and then which was grinded, polished and etched with 4 wt.% nitric acid alcohol solution for metallographic microstructure observation by Leica5000 type metallographic microscope.

The contents of the microstructure were measured by node method, and the ferrite grain size was measured by using the method of cutting line measurement.

The Charpy impact tests for V-notch specimens were performed at -40, 20, 0 °C and room temperature (25 °C), respectively, then the tensile fracture morphologies of which were observed by HITACHIS-4500 scanning electron microscopy (SEM). The second-phase precipitates were obtained by electrolytic extraction, which were analyzed by XRD-7000 X-ray diffraction (XRD) apparatus to get quantitative analysis results. Moreover, the morphology of second phase precipitates was observed by Tecnai20 transmission electron microscopy (TEM).

## 3. RESULTS

### 3.1. Mechanical properties

The tensile curves with different V-Nb microalloyed treatment for 1# and 2# samples are presented in Fig. 2, which exhibit similar standard tensile behavior with obvious yield plateau appearing, showing higher mechanical property compared with lower grade strength rebars.

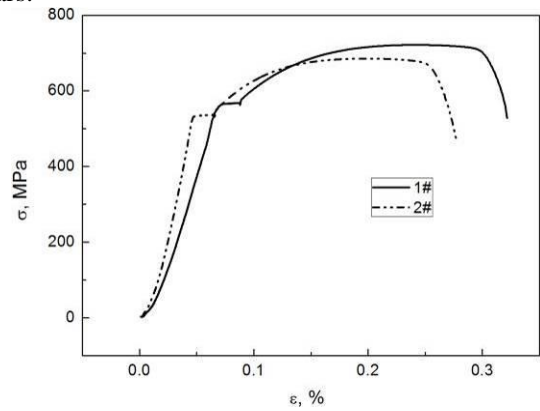


**Fig. 2.** True stress-true strain curves with different V-Nb microalloyed treatment

The mechanical properties of tested steels from tensile curves are summarized in Table 2. As it is observed, the mechanical properties of rebars are well controlled with yield strength more than 500 MPa due to strengthening effect of Nb and V addition. The yield strength (*ReL*), ultimate tensile strength (*Rm*), the tensile elongation to fracture (*A*) and total elongation (*Agt*) were higher than the lowest limits from Chinese GB/1499.2-2007, showing strong anti-risk ability. For the seismic performance, the ratio value of *Rm/ReL* is higher than 1.25 and the ratio value of *ReL<sub>real</sub>/ReL* is below 1.30, which satisfies the seismic requirements by Chinese GB/1499.2-2007 criterion.

**Table 2.** Mechanical properties of 500 MPa high-strength rebars by different V-Nb microalloyed process

Steel No.	<i>ReL</i> , MPa	<i>Rm</i> , MPa	<i>Rm/ReL</i>	<i>ReL<sub>real</sub>/ReL</i>	<i>Agt</i> , %	<i>A</i> , %
1#	545	710	1.30	1.09	12.5	21.5
2#	535	690	1.29	1.11	12.0	20.5

The SEM Micrographs of tensile fracture for 1# and 2# samples are presented in Fig. 3, in which it is

representative ductile fracture morphology with many small deep dimples distribution, indicating good plastic deformation performance.

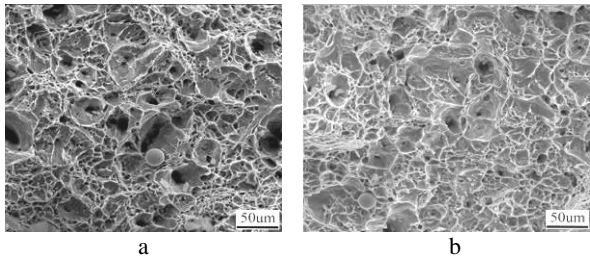


**Fig. 3.** SEM micrographs of tensile fracture for V-Nb microalloyed 500 MPa tested steels: a–1#; b–2#sample

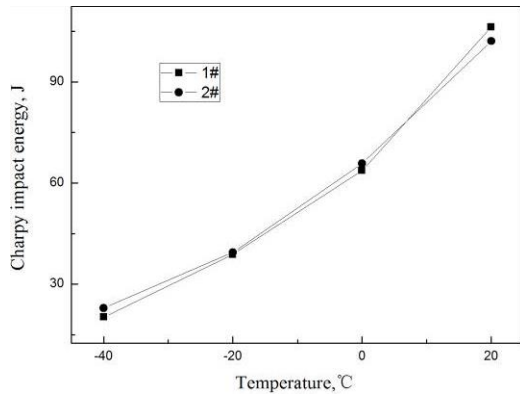


**Fig. 4.** Charpy impact energy tests for 1# and 2# samples with temperatures ranging from -40 to 20 °C

Fig. 4 shows the impact tests for 1# and 2# samples, it is obviously observed that the values of impact energy decreased with decrease of impact temperature. It is well known that the ductile-brittle transition temperature is located at the temperature with Charpy impact energy value of 27 J according to previous evaluation criterion [13, 14]. Thus, it can be inferred that the ductile-brittle

transition temperature of 1# and 2# specimens were lower than -30 °C at ductile-brittle with higher value than 27 J, indicating good impact toughness at low temperature.

### 3.2. Microstructure analysis

The microstructures of center and outer layer regions of transversal section for 1# and 2# samples are shown in Fig. 5 a–d. It is observed that white polygonal ferrite and dark lamellar pearlite were uniformly dispersed on matrix besides an amount of granular bainite formation. Moreover, more ferrite microstructure formed in outer layer region of transversal section than center region due to higher cooling intensity. Fig. 5 e–f shows that different rows of microstructure consisting refining ferrite and pearlite grains formed sequentially along the rolling direction, indicating that the microstructures were well controlled by controlled rolling and cooling technology. As shown in Table 3, different microstructure content and ferrite grain size for the center microstructure of transversal section of 1# and 2# samples were obtained.

**Table 3.** Quantitative analysis results of different microstructure contents and ferrite grain size for the center microstructure of transversal section of tested steels

Steel No.	Ferrite content, %	Pearlite content, %	Bainite content, %	Ferrite grains size, um	Ferrite grain grade
1#	51.0	38.4	10.8	7.2	11.0
2#	56.7	37.3	6.3	8.4	10.5

It is shown that the bainite contents of center microstructures of 1# and 2# are 10.8 % and 6.3 %, respectively. For the ferrite grains, the grain grade and grain size of 1# and 2# are 11.0, 10.5 and 7.2, 8.4 um, respectively, which exhibited favorable grain refining effect.

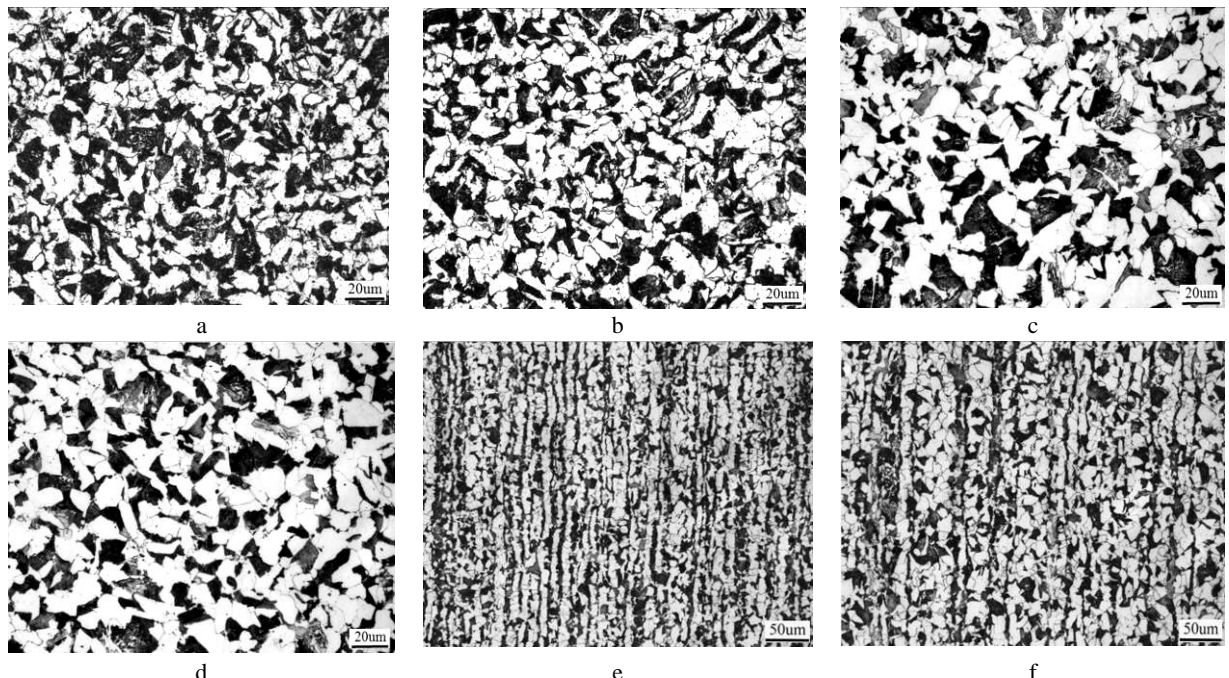


**Fig. 5.** Optical microstructure of 500 MPa high-strength rebars processed by V-Nb microalloyed and controlled cooling technology: a – the center of transversal section of 1#; b – the outer layer of transversal section of 1#; c – the center of transversal section of 2#; d – the outer layer of transversal section of 2#; e – longitudinal section of transversal section of 1#, f – longitudinal section of transversal section of 2#

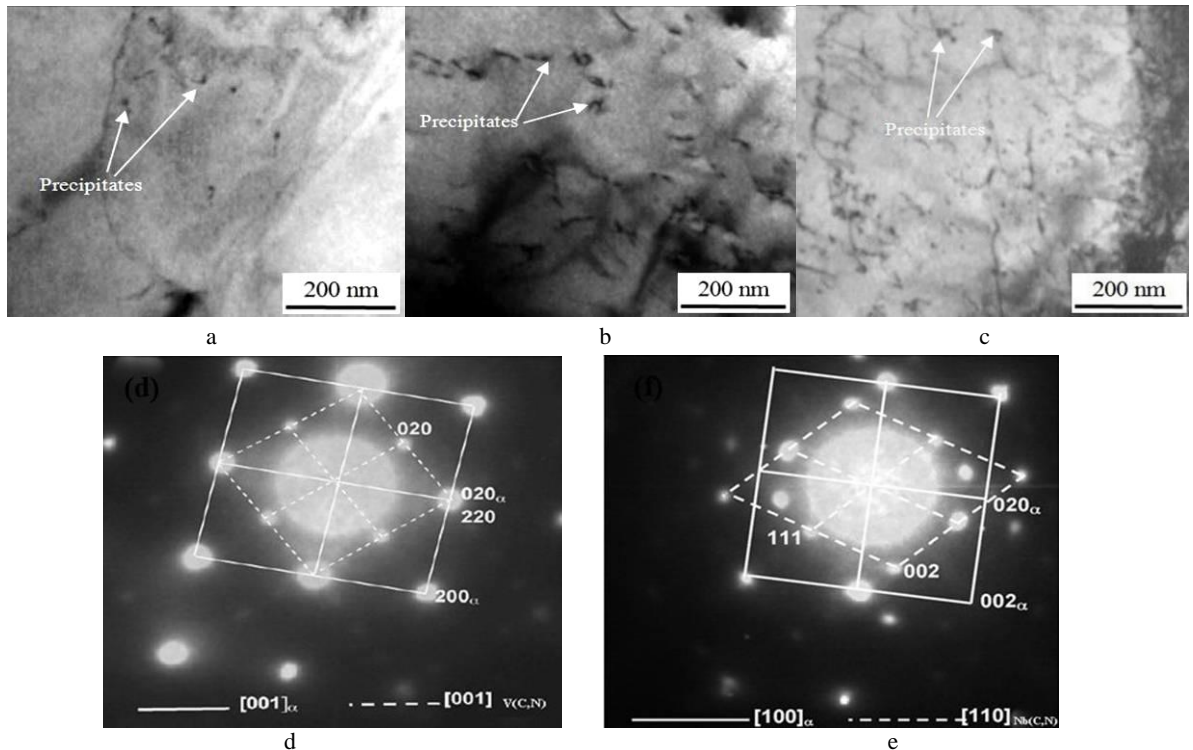


**Fig. 6.** TEM micrographs and diffraction patterns of second-phase precipitates for tested steels: a – precipitation at grain boundaries; b – precipitation on dislocations; c – precipitation in ferrite matrix; d – selected area diffraction (SAD) pattern of V(C,N) precipitates and e SAD pattern of Nb(C,N)

**Table 4.** Quantitative analysis results of second-phase precipitates for 1# sample

Contents of micro-alloying element M (V or Nb) in steel (wt.%)	MC precipitate			M(C,N) precipitate			Solution M	
	Content, wt.%	Ratio, %	Size, nm	Content, wt.%	Ratio, %	Size, nm	Content, wt.%	Ratio, %
V	0.029	0.003	10.35	10-30	0.021	72.41	5-25	0.005
Nb	0.019	0.002	10.53	10-30	0.013	68.42	5-20	0.004

### 3.3. Precipitates

The TEM morphology of second-phase precipitates for tested steels are shown in Fig. 6, in which it is observed that a large number of fine precipitates were dispersed on ferrite matrix, grain boundary and dislocation lines (Fig. 6 a–c).

These precipitates are identified as vanadium carbonitride (V(C,N)) and Niobium carbonitride (Nb(C,N)) phases by selected area diffraction (SAD) patterns as shown in Fig. 6 d–e. Table 4 shows the quantitative analysis results of extracted second-phase precipitates for 1# sample by XRD analysis, in addition to some precipitation of VC and NbC with size of 10–30 nm, the amount of V(C,N) and Nb(C,N) precipitates ratio account for 72.41 and 68.42 %, respectively. These precipitates with fine size of 5–30 nm play an effective role to grain refinement and precipitation strengthening.

## 4. DISCUSSION

### 4.1. Solution and grain refinement strengthening

According to the expansion Hall-Petch formula [15], the relationship between yield strength and various strengthening methods is described as following

$$\sigma_y = \sigma_0 + \Delta\sigma_{ss} + \Delta\sigma_g + \Delta\sigma_p + \Delta\sigma_t, \quad (1)$$

where  $\sigma_y$  represents the yield strength, the crystal lattice resistance of ferrite  $\sigma_0$  is about 53 MPa.  $\Delta\sigma_{ss}$  is the solution strengthening increments,  $\Delta\sigma_g$  is fine grain strengthening increments,  $\Delta\sigma_p$  stands for precipitation strengthening increments,  $\Delta\sigma_t$  is phase transformation strengthening (microstructure strengthening) increments of pearlite or bainite. Therefore, in order better to explain the strengthening mechanism of tested steels to yield strength, the grain refinement strengthening, precipitation strengthening, solution strengthening and phase transformation strengthening need to be further investigated.

Solution strengthening is caused by flexible interaction due to matrix crystal lattice distortion taken up by solution atoms. The stress field caused by crystal lattice distortion can restrain dislocation movement and promote strength of rebar. The effect of solution strengthening is related to the type and content of alloy elements of steel. According to the following formula, the increment of solution strengthening ( $\Delta\sigma_{ss}$ ) can be calculated [16].

$$\alpha_{ss} = 4750[C] + 37[Mn] + 83[Si], \quad (2)$$

where the [ ] represents the mass fraction of alloy elements (wt.%), but the effect of carbon content on solution strengthening may not be included in the C-Mn steel [17]. Therefore, the solution strengthening increments in this work can be expressed as following

$$\Delta\sigma_{ss} = 37[Mn] + 83[Si]. \quad (3)$$

The calculated solution strengthening increments of 1<sup>#</sup> and 2<sup>#</sup> samples are 88 and 92 MPa, respectively by the formula from the chemical composition of table 1, the contribution ratio of which to the yield strength are 15.8 and 17.1 %, respectively. It is similar to commonly accepted solution strengthening value.

It is well known that the grain refinement strengthening is the only way to increase both strength and toughness in steel [18]. The grain boundaries refinement prevents dislocation movement, thus increases the yield strength of rebar. Meanwhile, the amount of grain boundaries increase can prevent crack propagation, reducing the number of dislocation pileup and lowering the stress concentration and segregation concentration of impurity elements, so as to improving toughness of steel. The grain refinement strengthening increment of rebars can be given by the Hall-Petch equation

$$\Delta\sigma_g = k \cdot d^{-1/2}, \quad (4)$$

where  $k$  is the proportional constant, the value of which is 17.5 MPa.mm<sup>1/2</sup>,  $d$  is the diameter of ferrite grain (mm). Thus, the calculated grain refinement strengthening increments of 1<sup>#</sup> and 2<sup>#</sup> samples are 206 and 192 MPa respectively from the data in table 2, and the contribution ratio of which to the yield strength are 37.1 and 35.8 %, respectively. Therefore, the strength of tested steels can be markedly improved by grain refinement, which agreed well with previous report [8].

The effect of grain refinement of tested steels was related to Nb(C,N) and V(C,N) precipitates during deformation. As shown in Fig. 5 and Table 3, a large number of small and dispersive Nb(C,N) and V(C,N) precipitates induced by strain in rolling process can effectively retard austenite recrystallization and further refine the microstructure by suppressing austenite ( $\gamma$ ) and ferrite ( $\alpha$ ) grain coarsening during cooling. Meanwhile, lower the finish-rolling temperature in this study is beneficial to promote more deformation band formation in deformed austenite, which can enhance microstructure refinement during  $\gamma \rightarrow \alpha$  phase transformation by increasing  $\gamma \rightarrow \alpha$  nucleation sites and rates [19, 20].

## 4.2. Precipitation and microstructure (phase transformation) strengthening

The precipitation strengthening mechanism can be divided into two kinds: Orowan mechanism and cutting through mechanism [21]. The two mechanisms have a close relationship with particle volume fraction ( $f$ ) and particle size ( $d$ ), the relationship between the precipitation strengthening increment and  $f$ ,  $d$  can be expressed as follows

$$\sigma_{po} \propto f^{1/2} d^{-1} \cdot \ln d. \quad (5)$$

For the cutting through mechanism, the relationship between precipitation strengthening increment and  $f$ ,  $d$  can be expressed as follows

$$\sigma_p \propto f^{1/2} d^{1/2}. \quad (6)$$

The Orowan mechanism is taken as main precipitation strengthening method because the size of most microalloying carbonitride particles is larger than the critical transformation size in steels. According to orowan mechanism of microalloying carbonitride precipitation strengthening, the precipitation strengthening increments of tested steel can be taken by Orowan-Ashby equation as follows [22]

$$\Delta\sigma_p = (0.538Gb f_v^{1/2} / x) \ln(x/2b), \quad (7)$$

where  $\sigma_p$  is yield strength increment (MPa), the value of shear modulus ( $G$ ) is 81600 MPa for iron matrix, the value of Burger vector ( $b$ ) is 0.248 nm for ferrite,  $f_v$  and  $x$  are volume fraction and diameter of precipitates, respectively [23]. Thus, the precipitation strengthening effect is proportional to volume fraction of the second-phase carbonitride and inversely proportional to carbonitride particle size. The smaller particle size, the greater strengthening effect can be obtained. For the tested steels, a large number of small and dispersive carbonitride formed in the ferrite matrix, grain boundaries and on dislocation. For 1<sup>#</sup> tested steel in Table 3, the size of precipitation V(C,N) is 5 – 25 nm and the precipitation ratio is 72.41 %, the size of precipitation Nb(C,N) is 5 – 20 nm and the precipitation ratio is 68.42 %. As a result, the calculated precipitation strength increment of 1<sup>#</sup> sample is about 114 – 116 MPa and the contribution ratio to yield strength is 21.1 %, having significant precipitation strength effects to rebar, which is corresponding to previous study [2–4].

At present, there are two algorithms for calculating microstructure strengthening increments, one of which is obtained by the tested yield strength subtracting other strength increments, while the other is to obtain microstructure strengthening increment relationship by regression fitting from experimental data. In this study, the contribution in increment of microstructure strengthening to yield strength by the first algorithms is calculated under the form

$$\Delta\sigma_t = \Delta\sigma_{test} - \Delta\sigma_0 - \Delta\sigma_{ss} - \Delta\sigma_g - \Delta\sigma_p, \quad (8)$$

where  $\Delta\sigma_{test}$  is the real tested yield strength by tensile testing, the crystal lattice resistance of ferrite  $\sigma_0$  is about 53 MPa,  $\Delta\sigma_{ss}$ ,  $\Delta\sigma_g$  and  $\Delta\sigma_p$  are solution strengthening increment, grain refinement strengthening increment and precipitation strengthening increment, respectively. From above calculation equation, the microstructure strengthening increment of tested steel is measured about 90 MPa, and the contribution ratio to yield strength is 16.5 %. According to above microstructure analysis, the microstructures of tested steels consist of ferrite, pearlite and a small amount of bainite. The bainite microstructure formation can be attributed to Nb addition and controlled rolling and cooling technology using for rebar production, which will improve the strength of tested steel to some extent as a metastable phase. Compared with ferrite and pearlite microstructure, this complex phase microstructures

showed better strengthening effect [24].

### 4.3. Toughening mechanism

The plasticity and toughness of materials are determined by yield strength and the relative size of a crack nucleation stress and critical crack extension stress, which not always decreases with increase of strength [25]. For the tested steels, the solution strengthening is mainly caused by Si and Mn substitution, leading to small lattice distortion, which has little effect on the toughness. For precipitation strengthening, the ductile-brittle temperature increases and the elongation decreases with increasing yield strength, which is not conducive to improving plasticity and toughness of steel. However a large number of small and dispersive V(C,N) and Nb(C,N) particles formed in tested steel also contributed to strengthening effect of grain refinement, making the strength and toughness of steel simultaneously improved. The ductile-brittle transition temperature represents the toughness of the material, and the relations between ductile-brittle transition temperature  $T_c$  and grain size of rebar are expressed as follows

$$T_c = A - B \cdot \ln d^{-1/2}, \quad (9)$$

where  $A$  is the effect of other factors on ductile-brittle transition temperature except for grain refinement,  $B$  is the proportional constant, the value of which is about  $11.5 \text{ }^{\circ}\text{C}$  ( $\text{mm}^{1/2}$ ),  $d$  is the grain size. It can be inferred from the formula that the ductile-brittle transition temperature become lower while the grain size get finer. Impact testing results showed that tested steels have good impact toughness at low temperature with ductile-brittle transition temperature lower than  $-30 \text{ }^{\circ}\text{C}$ . A large number of small and dispersive carbonitride precipitation formed in tested steel, which can inhibit grain coarsening during rapid deformation cooling procedure. As shown in Table 2, quantitative analysis results of ferrite grain size are in the range of  $7 - 8.5 \mu\text{m}$ , corresponding to grain refinement effect. Therefore, from Eq. 9, it can be calculated that grain refinement makes impact transition temperature decrease a lot, which can make up for impairing effect of other strengthening mechanisms to toughness. However, more microalloyed vanadium addition can impair grain refinement effect [9].

## 5. CONCLUSIONS

The strengthening and toughening mechanism of 500MPa V-Nb microalloyed anti-seismic rebars in this paper was investigated. The conclusions of this study can be summarized as following:

1. The complex phase microstructures of 500 MPa high-strength rebars were produced by V-Nb microalloyed and controlled rolling and cooling technology. The plasticity and low-temperature toughness enhancement were mainly attributed to ferrite grain refinement improvement.
2. The degree of grain refinement was obtained by measurement of ferrite microstructure grade, which contribute to the grain refinement strengthening. The calculated precipitation strength increment from V(C,N) and Nb(C,N) precipitates revealed that the

tested steel has significant precipitation strength effects to rebar.

3. The mechanical performance of the steels was improved by grain refinement strengthening, precipitation strengthening and microstructure strengthening. The contribution ratio of grain refinement strengthening to yield strength of 1# and 2# tested steels are 37.1 and 35.8 % respectively, which revealed the best strengthening effect. Moreover, a small amount of bainite formation can improve the yield strength with about 16.5 % microstructure strengthening increment.

### Acknowledgment

This work is financially supported by the National Natural Science Foundation of China (Grant No. 51261009), Science and Technology Projects of Yunnan Province, PR China (No. 2009BA008), School Talent Project of Kunming University of Science and Technology (No.14118575).

### REFERENCES

1. Yang, C.F. Recent Developments of High Strength Rebars for Building *Iron & Steel* 45 (11) 2002: pp. 1 – 11.
2. Hong, S.G., Kang, K.B., Park, C.G. Strain-Induced Precipitation of NbC in Nb and Nb-Ti Microalloyed HSLA Steels *Scripta Materialia* 46 2002: pp. 163 – 168. [http://dx.doi.org/10.1016/S1359-6462\(01\)01214-3](http://dx.doi.org/10.1016/S1359-6462(01)01214-3)
3. Thomson, S.W., Krauss, G. Precipitation and Fine Structure in Medium-Carbon Vanadium and Vanadium/Niobium Microalloyed Steels *Metallurgical Transactions* 20 1989: pp. 2279 – 2288. <http://dx.doi.org/10.1007/BF02666663>
4. Hong, S.G., Jun, H.J., Kang, K.B., Park, C.G. Evolution of Precipitates in the Nb-Ti-V Microalloyed HSLA Steels During Reheating *Scripta Materialia* 48 2003: pp. 1201 – 1206. [http://dx.doi.org/10.1016/S1359-6462\(02\)00567-5](http://dx.doi.org/10.1016/S1359-6462(02)00567-5)
5. Shanmugam, S., Ramisetti, N., Misra, R.D.K., Hartmann, J., Jansto, S. G. Microstructure and High Strength-toughness Combination of a New 700 MPa Nb-Microalloyed Pipeline Steel *Materials Science Engineering A* 478 2008: pp. 26 – 37. <http://dx.doi.org/10.1016/j.msea.2007.06.003>
6. Reip, C.P., Shanmugam, S., Misra, R.D.K. High Strength Microalloyed CMn (V-Nb-Ti) and Mn(V-Nb) Pipeline Steels Processed Through CSP Thin-slab Technology: Microstructure, Precipitation and Mechanical Properties *Materials Science Engineering A* 424 2006: pp. 307 – 317. <http://dx.doi.org/10.1016/j.msea.2006.03.026>
7. Anumolu, R., Ravi Kumar, B., Misra, R.D.K. On the Determining Role of Microstructure of Niobium-Microalloyedsteels with Differences in Impact Toughness *Materials Science Engineering A* 491 2008: pp. 55 – 61.
8. Hulkka, K. The Role of Niobium in Cold Rolled Trip Steel *Materials Science Forum* 473 2005: pp. 91 – 102. <http://dx.doi.org/10.4028/www.scientific.net/MSF.473-474.91>
9. Sankaran, S., Sarma, V.S., Padmanabhan, K.A. Low Cycle Fatigue Behaviour of a Multiphase Microalloyed Medium Carbon Steel: Comparision Between Ferrite-pearlite and Quenched and Tempered Microstructures *Materials Science Engineering A* 345 2003: pp. 328 – 335.

10. **Tan, W., Han, B., Wang, S. Z.** Effect of TMCP Parameters on Microstructure and Mechanical Properties of Hot Rolled Economical Dual Phase Steel in CSP. *Journal of Iron and Steel Research International* 19 2012: pp. 37–41. [http://dx.doi.org/10.1016/S1006-706X\(12\)60124-1](http://dx.doi.org/10.1016/S1006-706X(12)60124-1)
11. **Wang, J. J., Fang, H. S., Yang, Z. G.** Fine Structure and Formation Mechanism of Bainite in Steels. *ISIJ International* 35 1995: pp. 992–1000.
12. **Riccardo, R., Carlo, M., Roberto, V.** Effect of Coiling Temperature on Formability and Mechanical Properties of Mild Low Carbon and HSLA Steels Processed by Thin Slab Casting and Direct Rolling. *Journal of Iron and Steel Research International* 47 2007: pp. 1204–1213.
13. **Erasmus, L. A., Pussegoda, L. N.** The Strain Aging Characteristics of Reinforcing Steel with a Range of Vanadium Contents. *Metallurgical Transactions A* 11 1980: pp. 231–237.
14. **Laurito, D. F., Baptista, C., Torres, M. A. S., Abdalla, A. J.** Microstructural Effects on Fatigue Crack Growth Behavior of a Microalloyed Steel. *Procedia Engineering* 2 2010: pp. 1915–1925.
15. **Misra, R. D. K., Weatherly, G. C., Hartmann, J. E., Boucek, A. J.** Ultrahigh Strength Hot Rolled Microalloyed Steels: Microstructural Aspects of Development. *Materials Science Technology* 17 2001: pp. 1119–1129. <http://dx.doi.org/10.1179/026708301101511040>
16. **Cao, J. C., Liu, Q. Y., Yong, Q. L.** Effect of Niobium on Microstructure and Strengthening Mechanism of HSLA Steel. *Iron Steel* 41 2006: pp. 60–63.
17. **Yang, C.F., Wang, Q.** Research Development and Production of V-N Microalloyed High-strength Rebars for Building in China. *Journal of Iron and Steel Research International* 15 2008: pp. 81–86.
18. **Eghbali, B., Abdollah-Zadeh, A.** Influence of Deformation Temperature on the Ferrite Grain Refinement in a Low Carbon Nb-Ti Microalloyed Steel. *Journal of Materials Processing Technology* 180 2006: pp. 44–48. <http://dx.doi.org/10.1016/j.jmatprotec.2006.04.018>
19. **Hong, S.C., Lee, K.S.** Influence of Deformation Induced Ferrite Transformation on Grain Refinement of Dual Phase Steel. *Materials Science Engineering A* 323 2002: pp. 148–159.
20. **Hodgson, P.D., Hickson, M.R., Gibbs, R.K.** Ultrafine Ferrite in Low-carbon Steel. *Scripta Materialia* 40 1999: pp. 1179–1184.
21. **Charieux, M., Poole, W.J., Militzer, M.** Precipitation Behavior and its Effects on Strengthening of an HSLA Nb/Ti Steel. *Metallurgical and Materials Transsections* 32 2001: pp. 1632–1635.
22. **Cao, J.C., Zhao, D.W., Chen, W., Shi, Z.** Strengthening Mechanisms and Microstructure of Vanadium and Nitrogen Microalloyed High Strength Seismic Rebar. *Advanced Materials Research* 450–451 2012: pp. 600–604.
23. **Gladman, T.** Precipitation Hardening in Metals. *Materials Science Technology* 15 1999: pp. 30–36. <http://dx.doi.org/10.1179/026708399773002782>
24. **Park, J.S., Lee, Y.K.** Nb (C,N) Precipitation Kinetics in the Bainite Region of a Low-carbon Nb-microalloyed Steel. *Scripta Materialia* 57 2007: pp. 109–112.
25. **Yong, Q.L., Ma, M.T., Wu, B.G.** Physical and Mechanical Metallurgy for Microalloying Steel, Springer, Beijing, 1989: pp. 304–319.